SCIENTIA MARINA 80(2)
June 2016, 247-259, Barcelona (Spain)
ISSN-L: 0214-8358
doi: http://dx.doi.org/10.3989/scimar.04391.07A

# Photo-physiological performance and short-term acclimation of two coexisting macrophytes (*Cymodocea nodosa* and *Caulerpa prolifera*) with depth

Fernando Tuya, Séfora Betancor, Federico Fabbri, Fernando Espino, Ricardo Haroun

Grupo en Biodiversidad y Conservación, IU-ECOAQUA, Universidad de Las Palmas de Gran Canaria, 35017, Las Palmas de G.C., Canary Islands, Spain. E-mail: ftuya@yahoo.es

**Summary**: Marine macrophytes are vertically distributed according to their ability to optimize their photosynthetic performance. We assessed the photo-physiological performance of the seagrass *Cymodocea nodosa* and the green seaweed *Caulerpa prolifera* at varying depth at Gran Canaria Island (Canary Islands, eastern Atlantic). The biomass of *C. nodosa* decreases with depth, while the opposite occurs for *C. prolifera*. Photochemical responses of both macrophytes were measured in shallow (5 m) and deep (20 m) waters at two times via chlorophyll *a* fluorescence and internal content of photoprotective pigments and antioxidant activity. We additionally carried out a reciprocal transplant experiment by relocating shallow and deep vegetative fragments of both macrophytes to assess their short-term photo-physiological acclimation. Overall, *C. nodosa* behaves as a 'light-plant', including a larger optimum quantum yield and $ETR_{max}$ under scenarios of high photosynthetically active radiation and a larger antioxidant activity. In contrast, *C. prolifera* is a 'shade-adapted' plant, showing a larger carotene content, particularly in shallow water. Deep-water *C. nodosa* and *C. prolifera* are more photochemically efficient than in shallow water. The alga *C. prolifera* shows a rapid, short-term acclimation to altered light regimes in terms of photosynthetic efficiency. In conclusion, decreased light regimes favour the photosynthetic performance of the green alga when both species coexist.

**Keywords**: macroalgae; seagrass; photoacclimation; photo-biology; photoprotection; Atlantic Ocean.

**Rendimiento foto-fisiológico y aclimatación a corto plazo de dos macrófitos coexistentes (*Cymodocea nodosa* y *Caulerpa prolifera*) con la profundidad**

**Resumen**: Los macrófitos marinos se distribuyen verticalmente de acuerdo a sus capacidades para optimizar su rendimiento fotosintético. Evaluamos el rendimiento foto-fisiológico de la fanerógama marina *Cymodocea nodosa* y el alga verde *Caulerpa prolifera* a diferentes profundidades en la isla de Gran Canaria (Islas Canarias, Atlántico oriental). La biomasa de *C. nodosa* decrece con la profundidad, mientras que para *C. prolifera* ocurre lo contrario. Las respuestas foto-químicas de ambos macrófitos se midieron en aguas someras (5 m) y profundas (20 m), en dos tiempos, a través de la fluorescencia de la clorofila *a* y los contenidos internos en pigmentos fotoprotectores y la actividad antioxidante. Además, ejecutamos un experimento de trasplante recíproco, recolocando fragmentos vegetativos de ambos macrófitos entre aguas someras y profundas para determinar su aclimatación a corto plazo. En general, *C. nodosa* se comporta como "planta de sol", con mayor rendimiento cuántico óptimo y $ETR_{max}$ bajo escenarios de alta radiación PAR y mayor actividad antioxidante. Contrariamente, *C. prolifera* es una "planta de sombra", mostrando mayor cantidad de carotenos, en particular a poca profundidad. Ejemplares profundos de ambos macrófitos son más eficientes foto-químicamente que los de aguas someras. El alga *C. prolifera* muestra una aclimatación rápida, a corto plazo, de su eficiencia fotosintética ante cambios en el régimen luminoso. En conclusión, regímenes depauperados lumínicamente favorecen el rendimiento fotosintético del alga verde.

**Palabras clave**: macroalgas; angiospermas; foto-aclimatación; foto-biología; fotoprotección; Océano Atlántico.

**Citation/Como citar este artículo**: Tuya F., Betancor S., Fabbri F., Espino F., Haroun R. 2016. Photo-physiological performance and short-term acclimation of two coexisting macrophytes (*Cymodocea nodosa* and *Caulerpa prolifera*) with depth. Sci. Mar. 80(2): 247-259. doi: http://dx.doi.org/10.3989/scimar.04391.07A

**Editor**: E. Ballesteros.

**Received**: December 18, 2015. **Accepted**: March 15, 2016. **Published**: June 8, 2016.

## INTRODUCTION

A variety of marine macrophytes (e.g. seagrasses and macroalgae) typically coexist in the same habitat; their distribution, however, may fluctuate under varying environmental conditions (e.g. light, nutrients), operating at a range of spatial and temporal scales (Lüning 1990). Marine macrophytes acclimate and adapt their photosynthetic apparatus to prevailing irradiance conditions (Betancor et al. 2015), which define species' niche requirements, including photoprotective mechanisms under high levels of UV and photosynthetically active radiation (PAR) (Häder et al. 1997). In turn, zonation patterns (or vertical distribution) of marine macrophytes are often related to their ability to resist high radiation stress (Hanelt 1998), e.g. upper-shore species are more resistant to elevated solar UV. In addition to their physiological responses, marine macrophytes show a certain degree of morphological flexibility that reflect long-term adaptations to varying environmental scenarios, including decreased light with depth in subtidal habitats (Olesen et al. 2002).

Under varying environmental scenarios, ecophysiological approaches that integrate estimates of light absorption efficiency, pigment contents and mechanisms to dissipate excess energy (Hanelt 1998) provide useful insight to assess changes in the distribution of marine macrophytes. This is particularly pertinent under scenarios of global change, in which the intensity and frequency of anthropogenic perturbations are increasing. For example, increasing turbidity in coastal areas alters the dominance and functioning of seascapes dominated by submersed vegetation, particularly those constituted by marine angiosperms (seagrasses) (Duarte et al. 2008, Silva et al. 2013). Understanding the physiological response of seagrasses and accompanying seaweeds to altered light regimes is therefore important (Collier et al. 2012).

*Cymodocea nodosa* (Ucria) Ascherson is a seagrass distributed across the entire Mediterranean Sea and the contiguous eastern Atlantic coasts, including the oceanic archipelagos of Madeira and the Canary Islands (Tuya et al. 2013a). Meadows constituted by *C. nodosa* are found on shallow sandy substrates throughout the Canary Islands (Barberá et al. 2005), supporting diverse invertebrate and fish assemblages (Tuya et al. 2006, Gardner et al. 2013, Tuya et al. 2013b). Across its distribution range, declines in the presence of *C. nodosa* may result in increases in the biomass of green algae, particularly those of the genus *Caulerpa*, including native (Lloret et al. 2005, García-Sánchez et al. 2012) and non-native species (Ceccherelli and Cinelli 1997). Species within the genus *Caulerpa* usually show rapid growth in high nutrient conditions (Lapointe et al. 2005). *Caulerpa prolifera* (Forsskål) J.V. Lamouroux is a native species from continental Europe, occurring in the Mediterranean Sea and the adjacent Atlantic Ocean. This coenocytic alga is a slow-growing, nitrophilic species with considerable morphological plasticity (Collado-Vides 2002, Malta et al. 2005), which may be connected with a large physiological plasticity when environmental conditions change (Malta et al. 2005). This alga has a prostrate axis (stolon) with rhizoids and upright axes (fronds) that are potentially independent units; the whole plant can regenerate after a frond or stolon is lost (Collado-Vides 2002). In the Canary Islands, the presence of *C. nodosa* has decreased in the last two decades, particularly in certain areas, correlating with a significant increase in the abundance of *C. prolifera* (Tuya et al. 2013a, Tuya et al. 2014). In this region, *C. nodosa* typically inhabits shallower waters than *C. prolifera*, though the two macrophytes can be found intermixed (Tuya et al. 2013a). In the Mar Menor (Mediterranean Sea), *C. nodosa* is mainly restricted to shallow-water areas (<1 m), while slightly deeper areas (2-5 m) are dominated by mono specific meadows of *C. prolifera* (García-Sánchez et al. 2012). It has been demonstrated that *C. nodosa* typically behaves as a 'light-plant', whereas *C. prolifera* behaves as a 'shade-plant', based on the differences in the way PAR is absorbed, the pigment composition, and the subsequent physiological mechanisms for dissipating excess light energy between the two macrophytes (Malta et al. 2005, García-Sánchez et al. 2012).

Previous studies have demonstrated morphological plasticity with depth of both *C. nodosa* (Olesen et al. 2002) and *C. prolifera* (Collado-Vives 2002). In this study, we assessed the photo-physiological performance of both macrophytes between a shallow and a deep-water stratum (5 vs 20 m depth), which involve significant changes in light regimes. This bathymetric gradient is considerably larger than those previously considered to compare the photo-physiology of both *C. nodosa* (0.4 vs 3.8 m, Olesen et al. 2002; 0.5 vs 5 m, García-Sánchez et al. 2012) and *C. prolifera* with depth (0.5 vs 5 m, García-Sánchez et al. 2012). We followed a two-step strategy. First, the photo-physiological performance—here quantified through photochemical responses via in vivo chlorophyll *a* fluorescence of photosystem II, as well as the contents in carotenes (widely recognized photoprotective pigments) and antioxidant activity—of the two macrophytes was directly measured from shallow and deep-water specimens at two times. Second, we carried out a reciprocal transplant experiment on the same two occasions by relocating shallow (5 m) and deep (20 m) vegetative fragments of both macrophytes. Subsequently, the photo-physiological performance of both macrophytes was assessed as an indicator of short-term acclimation to chronic changes in light regimes. Integration of results from both approaches provides insight on the photophysiological performance of these two co-occurring macrophytes and potential responses under altered light regimes.

## MATERIALS AND METHODS

### Reciprocal transplants: field work

This study was performed at Gran Canaria Island, a subtropical island in the centre of the Canary Islands (eastern Atlantic, 28°N). Sea surface temperature typically varies between 18°C in winter and 24ºC in

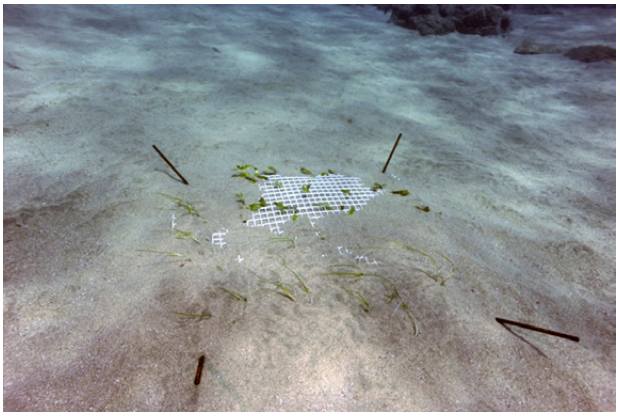

Fig. 1. – Experimental transplantation of vegetative fragments of *C. nodosa* and *C. prolifera* on a shallow-water soft bottom (5 m depth) at Gando Bay (Gran Canaria Island).

summer (Tuya et al. 2014). Vegetative fragments of *C. nodosa* (horizontal rhizomes ca. 10-15 cm long, including 5-7 shoots and associated leaves) and ramets of *C. prolifera*, including stolons, rhizoids and fronds (ca. 20-25 cm long), were collected by hand by SCUBA divers at 5 and 20 m depth at Gando Bay (27°55′49″N, 15°22′1″W). Neither species is typically found in shallower water in the study region, which is exposed to large oceanic swells that prevent long-term persistence. Collections of both macrophytes were immediately used to assess photochemical responses, as a way to infer their physiological status (see below). On the day of collection, we additionally carried out a reciprocal transplant experiment, in which 10-15 *C. nodosa* and *C. prolifera* vegetative fragments collected at 5 m were transplanted at 20 m depth and vegetative fragments collected at 20 m were transplanted at 5 m depth (hereafter called 'allochthonous' transplants). To control for potential artefacts during manipulations, *C. nodosa* and *C. proli fera* fragments from both depths were re-transplanted at the same depth (i.e. procedural controls, hereafter called 'autochthonous' transplants). All transplants were then subjected to the same manipulations. During transplants, the below-ground compartments of both macrophytes were gently buried inside the sediment by hand; to facilitate retention of below-ground tissues, plastic meshes covering horizontal rhizomes and stolons were secured to the bottom by metal stakes (Fig. 1). In all cases, the erect parts of both macrophytes (seagrass leaves and *C. prolifera* fronds) come out from the mesh to capture light with minimum perturbation. This experimental approach was repeated twice to evaluate the temporal consistency of results; the first started on 6 February 2014 and the second started on 15 May 2014. The duration of each transplant set varied slightly as a result of logistical constraints; on the first occasion (February 2014), transplants were maintained for 11 days; on the second occasion (May 2014), transplants were maintained for 14 days. During both periods, the amount of PAR reaching the bottom was measured by using Onset HOBO U12 4-channel external data loggers at 5 and 20 m depth, respectively.

## Bathymetric changes in macrophyte distribution and environmental drivers

To facilitate further interpretation of results, we described changes in the biomass of both *C. nodosa* and *C. prolifera* with depth at the study site. Samples (n=5) were collected through a 0.0125 $m^{-2}$ core at 5, 10, 15 and 20 m in Gando Bay at both sampling times. All vegetation was dried (24 h at 70°C) and the dry weight was calculated. Additionally, sediment samples (n=2 cores, ca. 100 g) were collected, in February 2014, at 5, 10, 15 and 20 m to work out differences in the mean particle diameter ($D_{50}$), the total N and P content and the organic matter content of sediments with depth. After thawing, sediment samples were sieved through a 0.5-mm sieve, and the fraction <0.5 mm was oven-dried at 90°C for 24 h. This fraction was then dry-sieved at 0.5 ϕ intervals, down to 1.0 ϕ (0.5 mm). The <0.5 mm fraction was freeze-dried and analysed on a Coulter LS130 laser sizer. The laser sizer results were combined with the dry sieve results to give the full particle size distribution. The method of Walkley and Black (1934) was used to calculate the organic matter content of sediments via rapid dichromate oxidation. Total N was determined following the Kjeldahl method (Bradstreet 1965) and total P was determined using a spectrophotometric method (Murphy and Riley 1962).

## Photochemical responses

At the start (initial collections) and at the end of the transplantation experiments, between n=6 and 8 *C. nodosa* leaves (12-15 cm long with no necrosis signs) and n=6 and 8 *C. prolifera* fronds (5-8 cm long) from each depth and manipulation treatment were used to estimate their photochemical status. In vivo chlorophyll *a* fluorescence of Photosystem II (PSII) was assessed through a portable pulse amplitude modulation fluorometer (Diving-PAM, Waltz GmbH, Germany). After 15 min of dark adaptation ('relaxed state'), the minimum (basal) fluorescence was measured ($F_o$) and the maximum fluorescence ($F_m$) was obtained immediately after applying a saturated pulse of actinic light (2,350 µmol photons $m^{-2}$ $s^{-1}$, 0.8 s). The optimum quantum yield was therefore calculated as $F_v/F_m=F_m–F_o/F_m$, which is an indicator of physiological stress (Maxwell and Johnson 2000). A rapid light curve (RLC) was initiated, involving 20 s of exposure to 9 successive irradiances, including 20, 66, 137, 224, 337, 469, 693, 942 and 1418 µmol photons $m^{-2}$ $s^{-1}$. RLCs were then obtained by calculating the electron transport rate (ETR) through the PSII for each level of actinic light through the formula:

$$\text{ETR (µmol electrons } m^{-2} s^{-1}) = (\Delta F/F'm) \times E \times A \times FII$$

where 'E' is the irradiance; 'A' is the absorptance of each macrophyte (0.88±0.02 for *C. nodosa* and 0.93±0.03 for *C. prolifera*, calculated using the method of García-Sánchez et al. 2012); and 'FII' is the fraction of chlorophyll associated with the PSII (0.5 for green seaweeds, according to Grzymski et al. 1997). RLCs

were fitted through the model provided by Jassby and Platt (1976) to obtain the initial slope of the curve ($\alpha_{ETR}$, i.e. the photosynthetic efficiency), the saturation irradiance ($E_k$) and the maximal ETR ($ETR_{max}$); the model of Platt and Gallegos (1980) was applied when photo-inhibition was detected.

### Carotenes and antioxidant activity

The carotene content was determined spectro-photometrically. The analyses were carried out by extracting pigments from plants (ca. 20 mg dry weight [DW], n=3) using 1 ml of saturation solution of acetone 90% + $C_4Mg_4O_{12}$ and maintaining them in darkness at 4°C for 12 h. After centrifugation at 4000 rpm for 20 min, each supernatant was used to measure carotenes in a spectrophotometer at an absorption of 480 and 750 nm. The carotene concentration, expressed as mg $g^{-1}$ DW, was calculated using the equation provided by Parsons and Strickland (1963).

Thalli of *C. nodosa* and *C. prolifera* (ca. 0.25 g FW, n=3) were ground with a mortar and a pestle in sand at 4°C and extracted overnight in centrifuge tubes with 2.5 ml of 80% (v/v) methanol. The mixture was centrifuged at 4000 rpm (30 min) and the supernatants were collected (Sigma 2-16PK, Göttingen, Germany). The DPPH (2,2-diphenyl-1-picrylhydrasyl) free-radical scavenging assay was carried out in triplicate, according to the method of Blois (1958). Briefly, 150 µL of each methanolic extract was mixed with 1.5 mL of 90% methanol and 150 µL of DPPH solution prepared daily at 1.27 mM. The reaction was complete after 30 min in darkness at room temperature, and the absorbance was registered at 517 nm. The calibration curve made with DPPH was used to calculate the remaining concentration of DPPH in the reaction mixture after incubation. Values of DPPH concentration (µM) were plotted against plant extract concentration (mg DW $mL^{-1}$) to obtain the $EC_{50}$ value (oxidation index), which represents the concentration of the extract (mg $mL^{-1}$) required to scavenge 50% of the DPPH in the reaction mixture. Ascorbic acid was used as a positive control.

### Statistical analyses

A three-way ANOVA tested for differences in the biomass of *C. nodosa* and *C. prolifera* across depth; the model included the factors 'Species' (fixed factor), depth (fixed factor) and 'Time' (random factor). Linear regression models tested whether the mean particle diameter ($D_{50}$), the mean total N and P content and the mean organic matter content of sediments varied with depth. To test for initial differences ('start' collections) in physiological responses between macrophytes (*C. nodosa* vs *C. prolifera*), depths (5 vs 20 m) and times (February vs May 2014), three-way ANOVAs were carried out. Each model incorporated the factors 'Species' (fixed factor), depth (fixed factor) and 'Time' (random factor). A three-way ANOVA tested separately for each macrophyte for significant differences in physiological responses between depths (two levels: 5 vs 20 m), times (two levels: February vs May) and the origin of the transplant (autochthonous = procedural control vs allochthonous) at the end of the transplants. The model incorporated the same factors as above, in addition to 'Origin' (fixed factor with two levels). For all ANOVAs, data were transformed to avoid heterogeneous variances (see Tables 1, 2 and 3 for specific transformations); Cochran's C test was used in this sense. If no transformation rendered homogeneous variances, the significance level was set at 0.01 rather than the 0.05 level to avoid increasing a type I error (Underwood 1997). Pairwise comparisons were carried out via Student-Newman-Keul (SNK) tests wherever necessary.

## RESULTS

### PAR patterns, sediment characteristics and vegetated biomass with depth

In February 2014, integrated mean PAR values at 5 m were ca. 2.57 times larger than at 20 m (Fig. 2A; means =124.50 vs 48.40 µ mol photons $m^{-2}$ $s^{-1}$), whereas in May 2014 they were ca. 2.24 times larger (Fig. 2B; means =251.72 vs 111.89 µ mol photons $m^{-2}$ $s^{-1}$). In general, maximum daily peaks in PAR increased from February to May 2014; for example, at 5 m, peaks increased from <1300 µmol photons $m^{-2}$ $s^{-1}$ to ~2000 µmol photons $m^{-2}$ $s^{-1}$. Sediments were dominated by fine sands at all depths (Appendix 1).

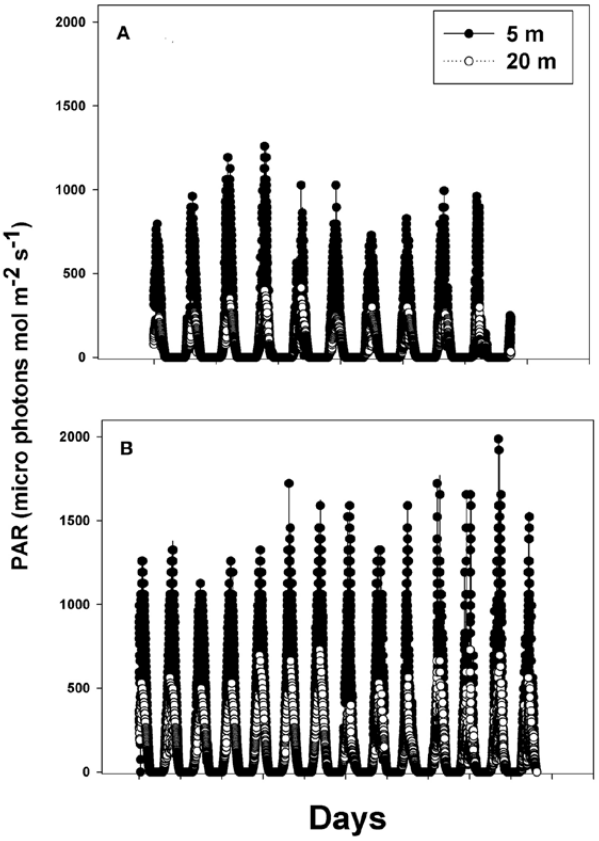


Fig. 2. – Incident PAR (mmol photons $m^{-2}$ $s^{-1}$) patterns through experimentation at 5 and 20 m depth in February (A) and May 2014 (B).

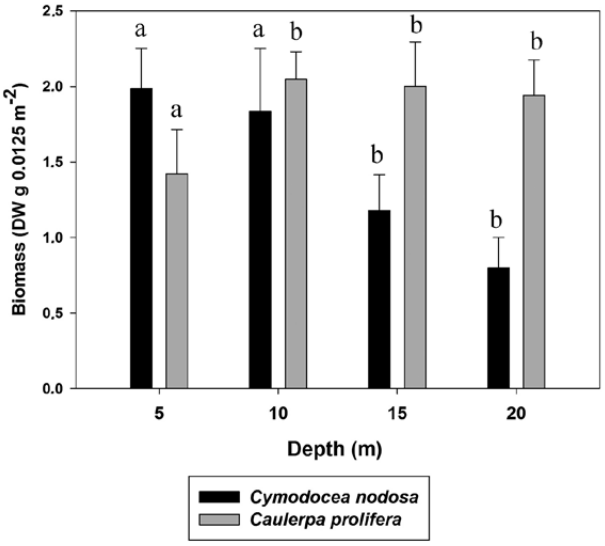


Fig. 3. – Changes in the biomass of *C. nodosa* and *C. prolifera* between depth strata at Gando Bay (Gran Canaria Island). Error bars are +SE of means (n=5). Times were pooled, as a result of lack of significant effects. Different letters above bars denote significant differences for each macrophyte.

The biomass of both macrophytes varied between depth strata following different trends ('Sp×De', $F_{3,64}$= 66.89, P<0.0001, Fig. 3). The biomass of the seagrass *C. nodosa* was larger at 5 and 10 m than at 15 and 20 m (SNK tests, Fig. 3). The biomass of *C. prolifera* showed a minimum at 5 m and similar values at 10, 15 and 20 m (SNK tests, Fig. 3). These patterns were consistent through times ('Species×Time', $F_{1,64}$=0.19, P=0.6657, 'De×Ti', $F_{3,64}$=0.11, P=0.9556), reinforcing the generality of these observations.

## Differences in initial photo-physiological responses

The seagrass *C. nodosa* showed a larger optimum quantum yield ($F_v/F_m$) than *C. prolifera*, particularly in May 2014 ('Ti×Sp', P=0.001, Table 1; Fig. 4), independently of depth (all terms involving 'De', P>0.05, Table 1; Fig. 4). Similarly, *C. nodosa* showed a significantly larger $ETR_{max}$ than *C. prolifera* in May 2014 ('Ti×Sp', P=0.0008, Table 1; Fig. 4), regardless of depth (all terms involving 'De', P>0.05, Table 1; Fig. 5). The seagrass *C. nodosa* also had a larger $\alpha_{ETR}$ than *C. prolifera* ('Sp', P<0.00001, Table 1; Fig. 6), which was particularly accentuated in May 2014 ('Ti×Sp', P=0.001, Table 1; Fig. 6). Both macrophytes were more photosynthetically efficient, i.e. larger $\alpha_{ETR}$ at 20 than 5 m depth ('De', P=0.0230, Table 1; Fig. 6). Appendix 2 includes means and SE of means of all photosynthetic parameters. The carotenoid content was significantly larger in *C. prolifera* than in *C. nodosa* ('Sp', P=0.001, Table 1; Fig. 7). While *C. nodosa* increased its carotene content from 5 to 20 m depth at both times, *C. prolifera* decreased it ('De×Sp', P<0.00001, Table 1; Fig. 7). The antioxidant activity of *C. nodosa* was significantly greater than that of *C. prolifera* ('Sp', P=0.0001, Table 1; Fig. 8).

Table 1. – Three-way ANOVAs testing the effect of 'Time' (Ti), 'Depth' (De) and 'Species' (Sp) on the optimum quantum yield of chlorophyll *a* fluorescence ($F_v/F_m$), the maximum electron transport rate ($ETR_{max}$), the photosynthetic efficiency calculated from ETR-E relationship ($\alpha_{ETR}$), the carotenoid content and the antioxidant activity ($EC_{50}$) of *Cymodocea nodosa* and *Caulerpa prolifera*. Significant values are highlighted in bold (P<0.05).

| | $F_v/F_m$ No transformation C=0.3781 (n.s.) | | | $ETR_{max}$ No transformation C=0.1811 (n.s.) | | | $\alpha_{ETR}$ No transformation C=0.3261 (n.s.) | | | Carotenoids Ln(x+1), C=0.5953 (P<0.05) | | | $EC_{50}$ Ln(x+1) C=0.7288 (P<0.01) | | |
|---|---|---|---|---|---|---|---|---|---|---|---|---|---|---|---|
| | MS | F | P | MS | F | P | MS | F | P | MS | F | P | MS | F | P |
| Ti | 0.0000 | 0.04 | 0.8502 | 14.8712 | 1.88 | 0.1898 | 0.0000 | 0.04 | 0.8502 | 0.0006 | 0.08 | 0.7753 | 0.0076 | 2.97 | 0.1039 |
| De | 0.0017 | 79.25 | 0.0712 | 2.5585 | 241.73 | **0.0409** | 0.0017 | 6.32 | **0.0230** | 0.0167 | 2.18 | 0.1592 | 0.0017 | 0.66 | 0.4298 |
| Sp | 0.0202 | 4.78 | 0.2732 | 452.34 | 3.32 | 0.3197 | 0.0202 | 76.48 | **0.0000** | 0.2114 | 27.63 | **0.0001** | 0.1466 | 57.35 | **0.0000** |
| Ti×De | 0.0000 | 0.08 | 0.7813 | 0.0106 | 0.00 | 0.9713 | 0.0000 | 0.08 | 0.7813 | 0.0103 | 1.34 | 0.2639 | 0.0091 | 3.57 | 0.0769 |
| Ti×Sp | 0.0042 | 16.01 | **0.0010** | 136.393 | 17.20 | **0.0008** | 0.0042 | 16.01 | **0.0010** | 0.0298 | 3.89 | 0.0660 | 0.0105 | 4.11 | 0.0596 |
| De×Sp | 0.0000 | 0.15 | 0.7660 | 4.5920 | 0.35 | 0.6601 | 0.0000 | 0.12 | 0.7364 | 0.3046 | 39.83 | **0.0000** | 0.0014 | 0.54 | 0.4727 |
| Ti×De×Sp | 0.0002 | 0.79 | 0.3868 | 13.1394 | 1.66 | 0.2163 | 0.0002 | 0.79 | 0.3868 | 0.0012 | 0.15 | 0.7003 | 0.0049 | 1.9 | 0.1871 |
| Residual | 0.0003 | | | 7.9290 | | | 0.0003 | | | 0.0076 | | | 0.0026 | | |

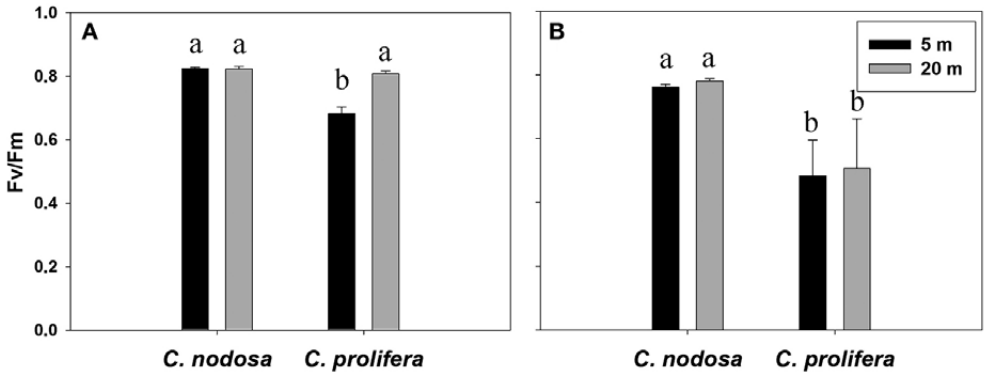


Fig. 4. – Optimum quantum yield of chlorophyll *a* fluorescence of the seagrass *Cymodocea nodosa* and the green alga *Caulerpa prolifera* at 5 and 20 m depth in February 2014 (A) and May 2014 (B). Error bars are +SE of means (n=6). Different letters above bars denote significant differences.

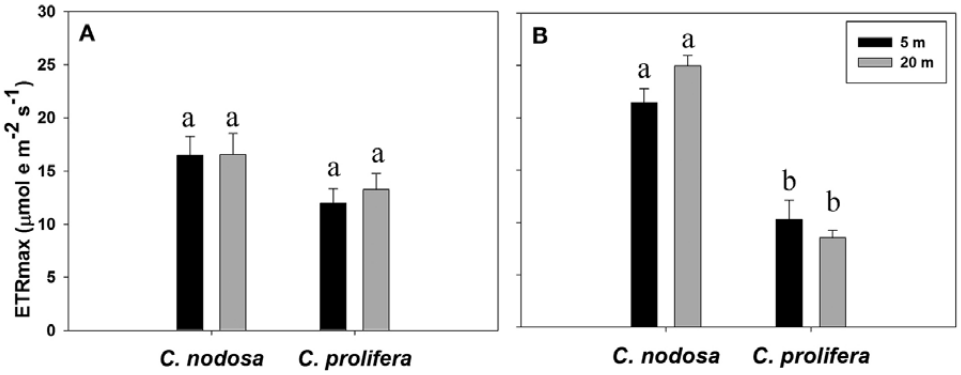


Fig. 5. – The maximum electron transport rate ($ETR_{max}$) of the seagrass *Cymodocea nodosa* and the green alga *Caulerpa prolifera* at 5 and 20 m depth in February 2014 (A) and May 2014 (B). Error bars are +SE of means (n=6). Different letters above bars denote significant differences.

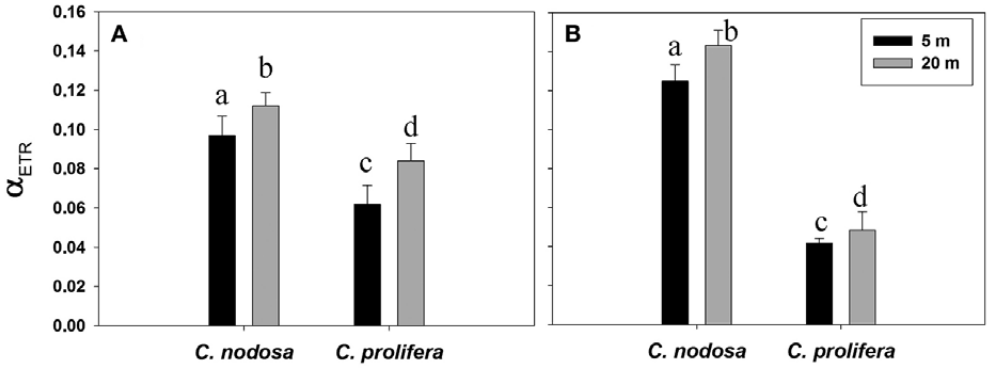


Fig. 6. – Photosynthetic efficiency calculated from ETR-E relationship ($\alpha_{ETR}$) of the seagrass *Cymodocea nodosa* and the green alga *Caulerpa prolifera* at 5 and 20 m depth in February 2014 (A) and May 2014 (B). Error bars are +SE of means (n=6). Different letters above bars denote significant differences.

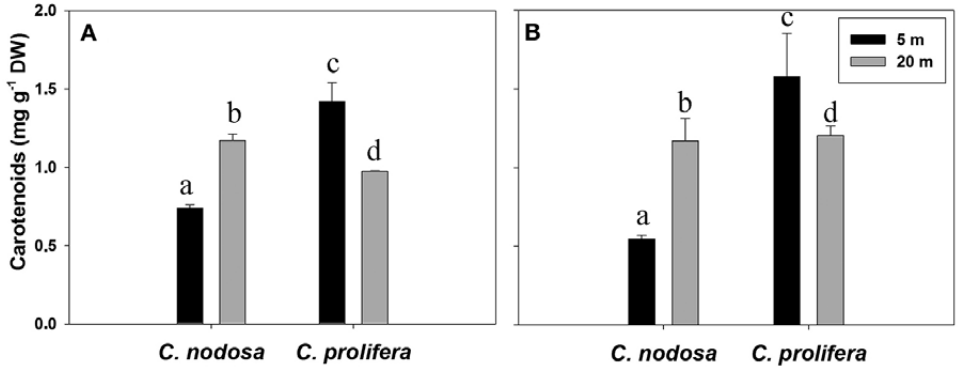


Fig. 7. – Carotenoids content of the seagrass *Cymodocea nodosa* and the green alga *Caulerpa prolifera* at 5 and 20 m depth in February 2014 (A) and May 2014 (B). Error bars are +SE of means (n=6). Different letters above bars denote significant differences.

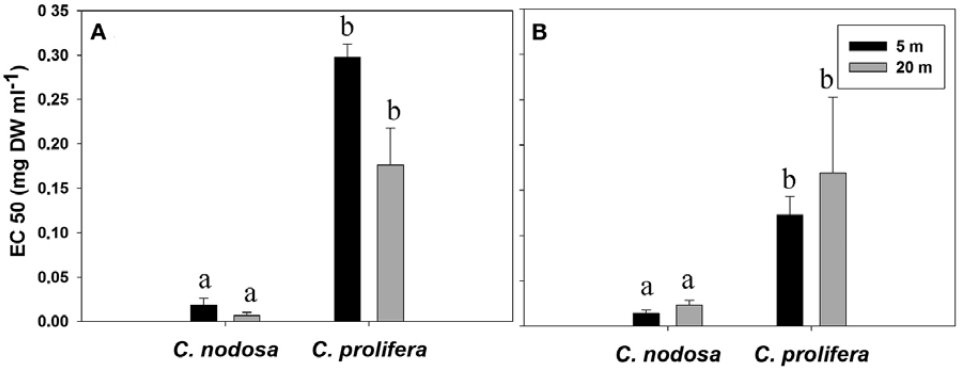


Fig. 8. – Antioxidant activity ($EC_{50}$ index) of the seagrass *Cymodocea nodosa* and the green alga *Caulerpa prolifera* at 5 and 20 m depth in February 2014 (A) and May 2014 (B). Error bars are +SE of means (n=6). The lower the $EC_{50}$ index, the larger the antioxidant activity. Different letters above bars denote significant differences.

Table 2. – Three-way ANOVAs testing the effect of 'Time' (Ti), 'Depth' (De) and 'Origin' (Or) on the optimum quantum yield of chlorophyll *a* fluorescence ($F_v/F_m$), the maximum electron transport rate ($ETR_{max}$), the photosynthetic efficiency calculated from ETR-E relationship ($\alpha_{ETR}$), the carotenoid content and the antioxidant activity ($EC_{50}$) of *Cymodocea nodosa* at the end of the reciprocal transplants. Significant values are highlighted in bold (P<0.05).

| | $F_v/F_m$ No transformation C=0.3084 (n.s.) | | | $ETR_{max}$ No transformation C=0.2602 (n.s.) | | | $\alpha_{ETR}$ No transformation C=0.2849 (n.s.) | | | Carotenoids No transformation C=0.1730 (n.s.) | | | $EC_{50}$ Ln(x+1) C=0.4114 (P<0.05) | | |
|---|---|---|---|---|---|---|---|---|---|---|---|---|---|---|---|
| | MS | F | P | MS | F | P | MS | F | P | MS | F | P | MS | F | P |
| Ti | 0.0217 | 23.00 | **0.0000** | 1866.33 | 94.49 | **0.0000** | 0.0272 | 29.07 | **0.0000** | 0.0038 | 0.18 | 0.6757 | 0.0268 | 10.59 | **0.0023** |
| De | 0.0001 | 0.08 | 0.8264 | 31.7493 | 231.81 | 0.0418 | 0.0004 | 4.32 | 0.2855 | 0.0674 | 0.19 | 0.7410 | 0.1944 | 3.33 | 0.3190 |
| Or | 0.0003 | 0.19 | 0.7411 | 7.5986 | 2.03 | 0.3899 | 0.0032 | 2.74 | 0.3460 | 0.0244 | 1.36 | 0.4510 | 0.0001 | 0.37 | 0.6531 |
| Ti×De | 0.0009 | 0.98 | 0.3275 | 0.1370 | 0.01 | 0.9341 | 0.0001 | 0.09 | 0.7650 | 0.3634 | 17.09 | **0.0002** | 0.0583 | 23.02 | **0.0000** |
| Ti×Or | 0.0015 | 1.57 | 0.2170 | 3.7498 | 0.19 | 0.6654 | 0.0012 | 1.26 | 0.2678 | 0.0179 | 0.84 | 0.3640 | 0.0003 | 0.12 | 0.7313 |
| De×Or | 0.0008 | 1.29 | 0.4592 | 11.1554 | 0.21 | 0.7268 | 0.0036 | 14.47 | 0.1637 | 0.1158 | 0.37 | 0.6539 | 0.0022 | 0.24 | 0.7086 |
| Ti×De×Or | 0.0006 | 0.68 | 0.4159 | 53.2945 | 2.70 | 0.1083 | 0.0003 | 0.27 | 0.6066 | 0.3169 | 14.90 | **0.0004** | 0.0090 | 3.57 | 0.0661 |
| Residual | 0.0009 | | | 19.7517 | | | 0.0009 | | | 0.0213 | | | 0.0025 | | |

## Differences in photo-physiological responses at the end of transplants

The optimum quantum yield of *C. nodosa* did not differ either between depth strata or between the origin of the vegetative fragment (all terms involving 'De' and 'Or', P>0.05, Table 2; Fig. 9A, B); significant differences only occurred between times ('Ti', P<0.00001, Table 2; Fig. 9A, B), including a decay in the optimum quantum yield in May in comparison with February (2014). The optimum quantum yield of *C. prolifera* varied between depths inconsistently from time to time ('Ti×De', P=0.0011, Table 3; Fig. 9C, D): in February 2014, the optimum quantum yield was larger for specimens collected at 20 than at 5 m, whereas in May 2014 no significant differences were detected (SNK tests, Fig. 9C, D). Thalli of *C. prolifera* increased the optimum quantum yield when transplanted from 5 to 20 m, while the opposite pattern was detected when thalli from 20 m were transplanted at 5 m (Fig. 9C, D). The $ETR_{max}$ of both macrophytes was larger in May than in February 2014 ('Ti', P<0.01, Tables 2 and 3; Fig. 10), regardless of depth and the origin of the vegetative fragments. The photosynthetic efficiency of *C. nodosa* ($\alpha_{ETR}$) varied exclusively between times; larger $\alpha_{ETR}$ values were observed in May (2014) ('Ti', P<0.00001, Table 2; Fig. 11A, B). Irrespective of times, however, *C. prolifera* showed a larger photosynthetic efficiency at 20 than at 5 m ('De', P=0.0066, Table 3; Fig. 11C, D). Thalli of *C. prolifera* increased their photosynthetic efficiency when transplanted from 5 to 20 m, while the opposite pattern was observed for thalli transplanted

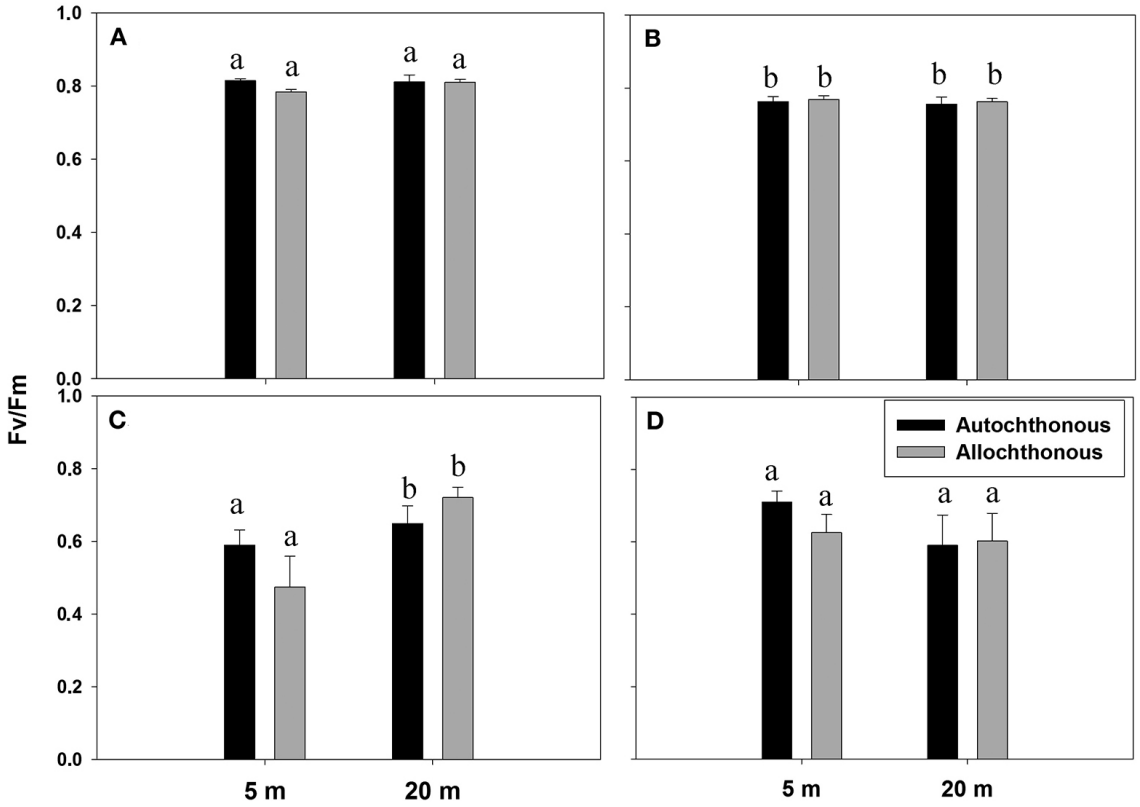


Fig. 9. – Optimum quantum yield of chlorophyll *a* fluorescence of the seagrass *Cymodocea nodosa* (A, B) and the green alga *Caulerpa prolifera* (C, D) at 5 and 20 m depth in February (A, C) and May 2014 (B, D). Error bars are +SE of means (n=6). Different letters above bars denote significant differences for each macrophyte.

Table 3. – Three-way ANOVAs testing the effect of 'Time' (Ti), 'Depth' (De) and 'Origin' (Or) on the optimum quantum yield of chlorophyll *a* fluorescence ($F_v/F_m$), the maximum electron tranposrt rate ($ETR_{max}$), the photosynthetic efficiency calculated from ETR-E relationship ($\alpha_{ETR}$), the carotenoid content and the antioxidant activity ($EC_{50}$) of *Caulerpa prolifera* at the end of the reciprocal transplants. Significant values are highlighted in bold (P<0.05).

| | $F_v/F_m$ No transformation, C=0.2621 (n.s.) | | | $ETR_{max}$ Ln(x+1), C=0.4585 (P<0.05) | | | $\alpha_{ETR}$ No transformation, C=0.3211 (n.s.) | | | Carotenoids No transformation, C=0.2425 (n.s.) | | | $EC_{50}$ Ln(x+1), C=0.5852 (P<0.01) | | |
|---|---|---|---|---|---|---|---|---|---|---|---|---|---|---|---|
| | MS | F | P | MS | F | P | MS | F | P | MS | F | P | MS | F | P |
| Ti | 0.0018 | 0.12 | 0.7319 | 1.5804 | 11.03 | **0.0019** | 0.0000 | 0.05 | 0.8324 | 0.7868 | 10.43 | **0.0025** | 2.9795 | 106.67 | **0.0000** |
| De | 0.0103 | 0.06 | 0.8520 | 0.6397 | 87.29 | 0.0679 | 0.0088 | 9165.25 | **0.0066** | 0.4619 | 8.67 | 0.2084 | 1.0153 | 0.27 | 0.6955 |
| Or | 0.0105 | 16.65 | 0.1530 | 0.0806 | 0.38 | 0.6493 | 0.0002 | 11.90 | 0.1796 | 0.6239 | 17.36 | 0.1500 | 0.0288 | 1.14 | 0.4787 |
| Ti×De | 0.1833 | 12.45 | **0.0011** | 0.0073 | 0.05 | 0.8222 | 0.0000 | 0.00 | 0.9522 | 0.0533 | 0.71 | 0.4058 | 3.7779 | 135.26 | **0.0000** |
| Ti×Or | 0.0006 | 0.04 | 0.8370 | 0.2136 | 1.49 | 0.2292 | 0.0000 | 0.07 | 0.7927 | 0.0359 | 0.48 | 0.4940 | 0.0252 | 0.90 | 0.3477 |
| De×Or | 0.0601 | 9.67 | 0.1981 | 0.0010 | 0.04 | 0.8742 | 0.0010 | 2.14 | 0.3816 | 0.0287 | 52.54 | 0.0873 | 0.0555 | 0.41 | 0.6363 |
| Ti×De×Or | 0.0062 | 0.42 | 0.5196 | 0.0238 | 0.17 | 0.6859 | 0.0005 | 1.77 | 0.1912 | 0.0005 | 0.01 | 0.9327 | 0.1344 | 4.81 | **0.0341** |
| Residual | 0.0147 | | | 0.1432 | | | 0.0003 | | | 0.0754 | | | 0.0279 | | |

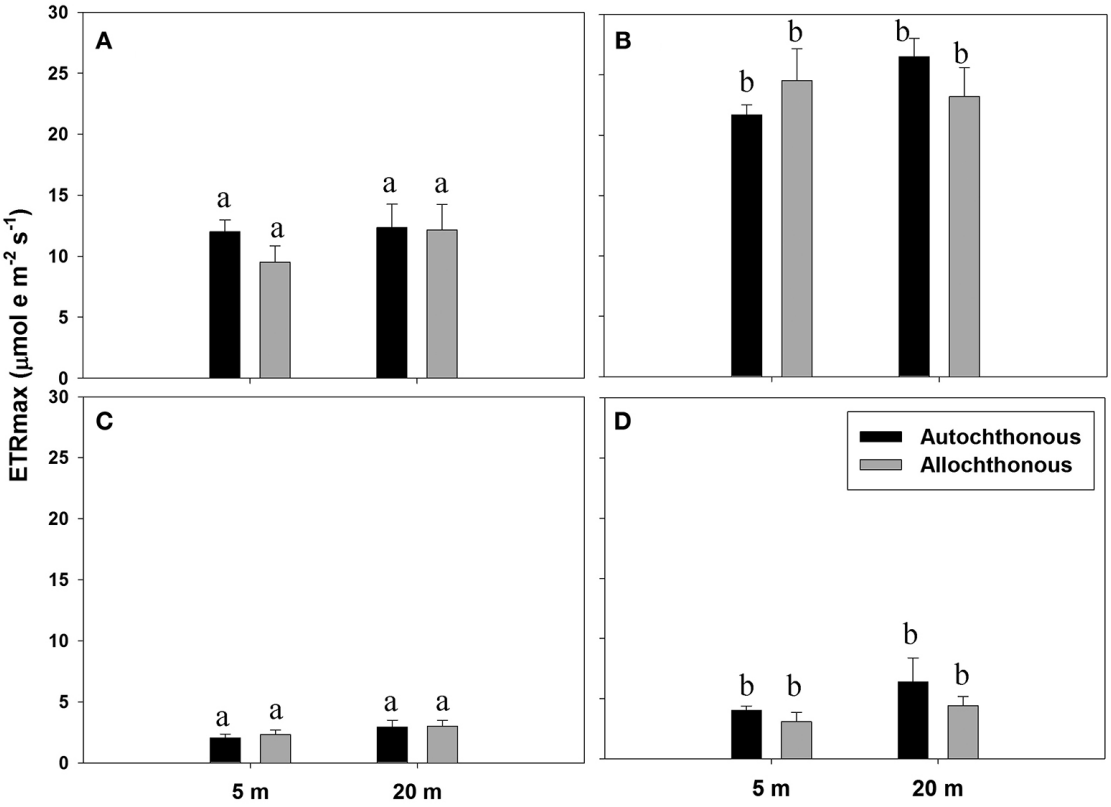


Fig. 10. – The maximum electron transport rate ($ETR_{max}$) of the seagrass *Cymodocea nodosa* (A, B) and the green alga *Caulerpa prolifera* (C, D) at 5 and 20 m depth in February 2014 (A, C) and May 2014 (B, D). Error bars are +SE of means (n=6). Different letters above bars denote significant differences for each macrophyte.

from 20 to 5 m (Fig. 11C, D); however, this pattern was not detected statistically (all terms involving 'De' and 'Or', P>0.05, Table 3; Fig. 11C, D). Appendix 3 includes means and SE of means of all photosynthetic parameters. The carotene content of *C. nodosa* differed between depths according to the origin of vegetative fragments from time to time ('Ti×De×Or', P=0.0004, Table 3; Fig. 12A, B). The magnitude of differences between depth levels depended on the origin ('De×Or', P=0.08, Table 3; Fig. 12C, D); differences in the carotene content between allochthonous and autochthonous fragments were more accentuated at 5 than at 20 m depth (SNK tests, Fig. 12C, D). The carotene content of *C. prolifera* differed exclusively between times ('Ti', P=0.00025, Table 3; Fig. 12C, D); a decrease in the carotene content was observed with increasing depth, but it was not statistically significant ('De', P=0.2084, Table 3; Fig. 12C, D). The antioxidant activity of both macrophytes varied between depths according to times, regardless of the origin of the vegetative fragments ('Ti×De', P<0.00001, Table 2 and 3; Fig. 13); differences in the antioxidant activity between 5 and 20 m depth were significant in February but not in May 2014 (SNK tests, Fig. 13).

## DISCUSSION

Our results have suggested a connection between the patterns of vertical distribution of the seagrass *C. nodosa* (i.e. decreased biomass with depth) and the green alga *C. prolifera* (i.e. increased biomass with depth) with their respective photochemical adaptations

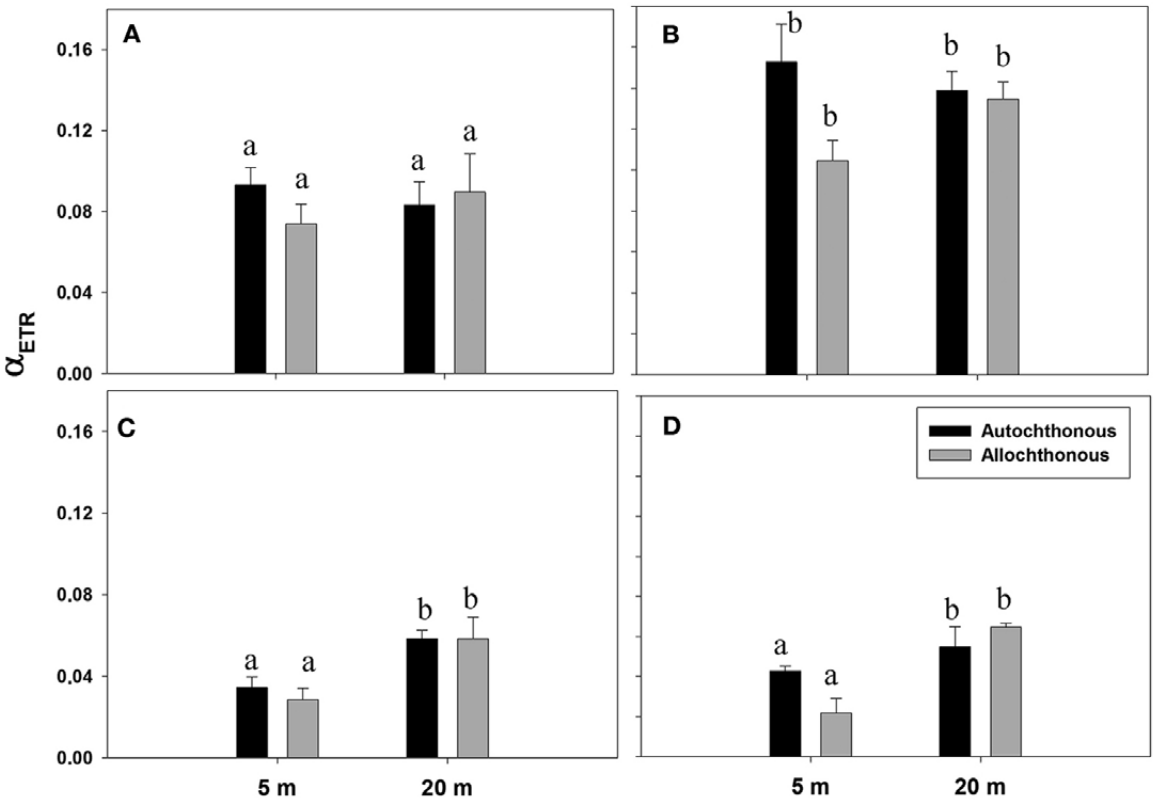


Fig. 11. – Photosynthetic efficiency calculated from ETR-E relationship ($\alpha_{ETR}$) of the seagrass *Cymodocea nodosa* (A, B) and the green alga *Caulerpa prolifera* (C, D) at 5 and 20 m depth in February 2014 (A, C) and May 2014 (B, D). Error bars are +SE of means (n=6). Different letters above bars denote significant differences for each macrophyte.

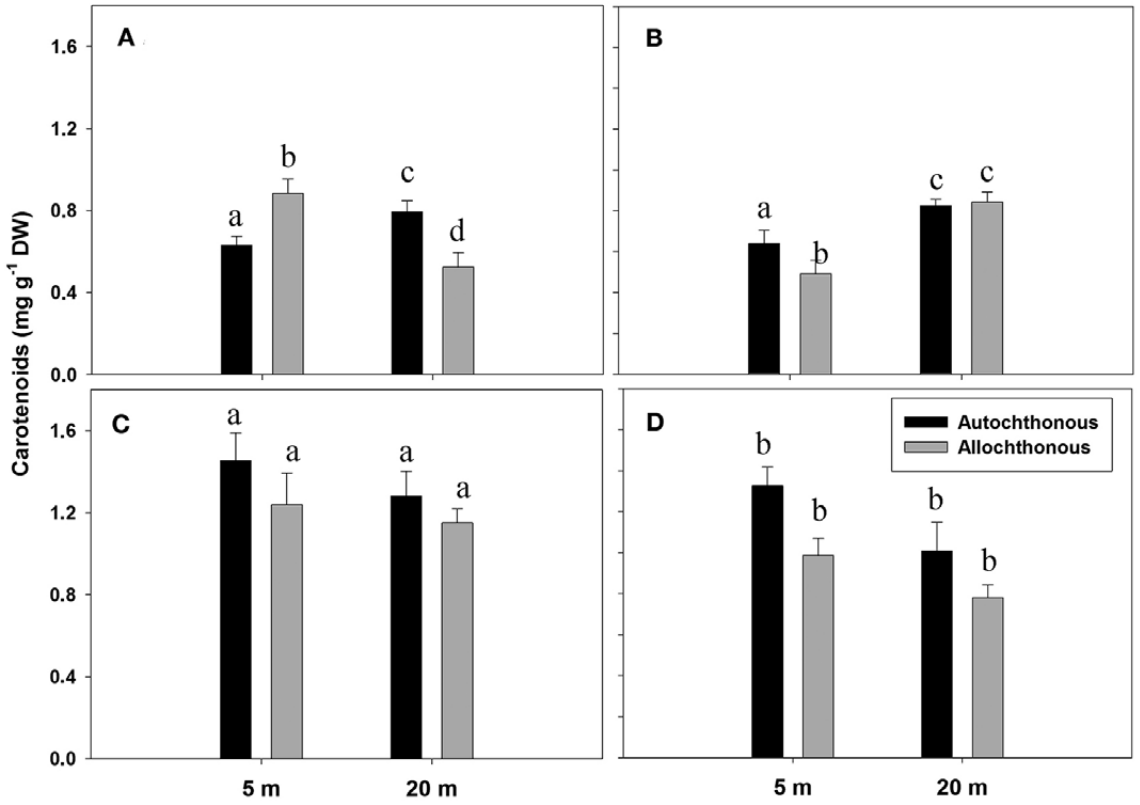


Fig. 12. – Carotenoids content of the seagrass *Cymodocea nodosa* (A, B) and the green alga *Caulerpa prolifera* (C, D) at 5 and 20 m depth in February 2014 (A, C) and May 2014 (B, D). Error bars are +SE of means (n=6). Different letters above bars denote significant differences for each macrophyte.

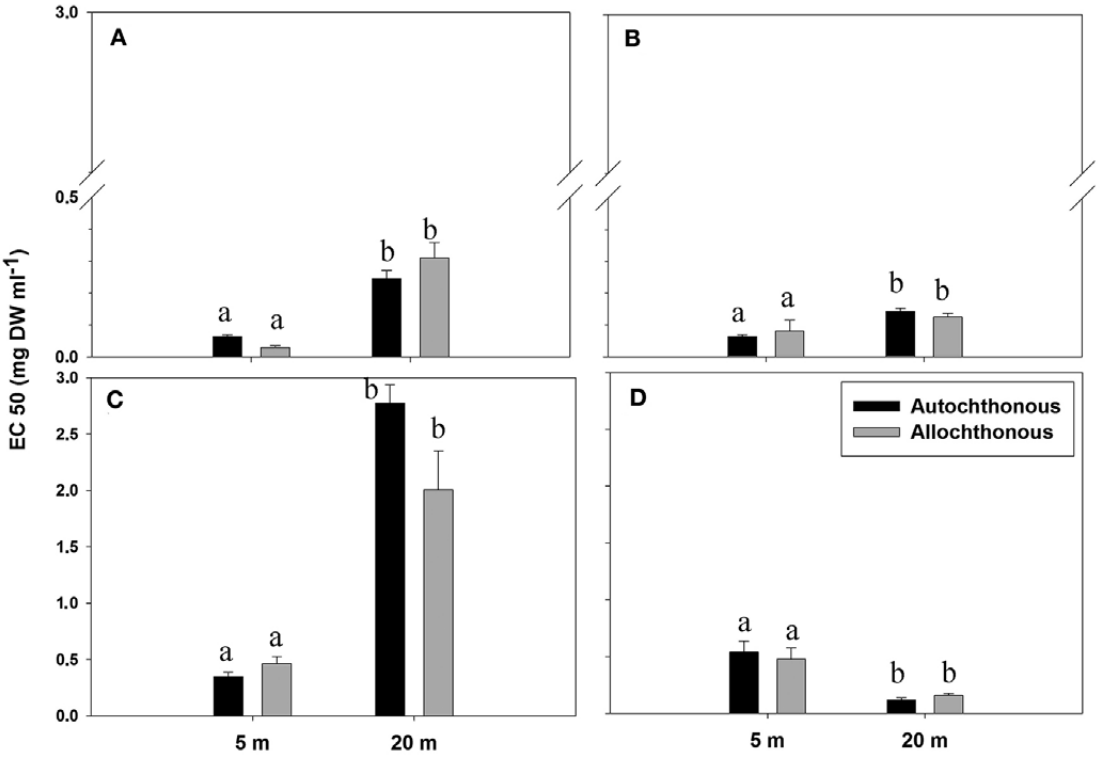


Fig. 13. – Antioxidant activity ($EC_{50}$ index) of the seagrass *Cymodocea nodosa* (A, B) and the green alga *Caulerpa prolifera* (C, D) at 5 and 20 m depth in February 2014 (A, C) and May 2014 (B, D). Error bars are +SE of means (n=6). The lower the $EC_{50}$ index, the larger the antioxidant activity. Different letters above bars denote significant differences for each macrophyte.

at the study site in Gran Canaria Island. Overall, *C. nodosa* behaves as a 'light-plant' relative to *C. prolifera*, which follows a 'shade-plant' pattern. This result is similar to that of a study comparing the photo-physiology of both macrophytes within a Mediterranean coastal lagoon (García-Sánchez et al. 2012). This outcome has implications in the way light is absorbed by both macrophytes, as well as in the quantity and quality of pigment contents, and in ways to ameliorate/dissipate the excess of light energy reaching photosynthetic tissues (Malta et al. 2005, García-Sánchez et al. 2012).

Our results demonstrated that the seagrass *C. nodosa* has a consistently larger optimum quantum yield ($F_v/F_m$), $ETR_{max}$ and photosynthetic efficiency than the green alga *C. prolifera*, particularly when PAR values are larger (May in comparison with February 2014). Evidence for this, moreover, was provided by direct measurements from collected thalli and at the end of the reciprocal transplants. This outcome is a clear indication of adaptation of the seagrass to larger irradiances and therefore optimization of light absorption in this time (May). Not surprisingly, this is particularly pertinent in this season, as this seagrass experiences rapid growth in spring-summer in the study region (Tuya et al. 2006), as well as in a range of sites across the Mediterranean Sea (e.g. Terrados and Ros 1992). Biomass accumulation (e.g. seagrass leaf growth and rhizome production) is metabolically based on increased photosynthetic rates and therefore high C demands. For *C. nodosa*, there is a positive correlation between gross primary production and ETR at the PSII, except under stressful conditions (e.g. low nutrients levels and very high PAR), as usually occurs for $C_4$ plants, including *C. nodosa* (Cabello-Pasini et al. 2015). In turn, decreased irradiances reaching the photosynthetic apparatus of *C. nodosa*, for example during fertilization events, negatively affect the production of photochemical energy by *C. nodosa* (Tuya et al. 2015). This seagrass showed increased photosynthetic potential ($ETR_{max}$) and photochemical energy conversion efficiency (α) under increased irradiances, i.e. at 5 in comparison with 20 m, and in May in comparison with February (2014). Under decreased irradiances (e.g. at 20 in comparison with 5 m depth), this seagrass shows increased photochemical energy conversion efficiency (α); this is a common strategy of marine angiosperms when they are subjected to chronic light deprivation (Collier et al. 2012), including *C. nodosa* (Silva et al. 2013).

The green alga *C. prolifera* has adapted its photosynthetic apparatus to prevailing light regimes, e.g. a larger photosynthetic efficiency at 20 than at 5 m depth. A similar pattern has been described for other *Caulerpa* species, such as *Caulerpa racemosa* in the Mediterranean Sea (Raniello et al. 2006, Bernardeau-Esteller et al. 2011). Not only deep-water (20 m depth) thalli of *C. prolifera* are more adapted to low irradiances: this alga also showed short-term acclimation under varying light regimes, i.e. when reciprocal transplants of vegetative fragments were carried out. When fragments from 5 m were relocated at 20 m depth, these fragment became more photo-chemically efficient (i.e. larger $F_v/F_m$ and $\alpha_{ETR}$), while the opposite occurred for deep-water fragments (20 m) relocated at 5 m. This photo-physiological versatility of *C. prolifera* provides

an additional, short-term advantage of this alga under varying environmental scenarios. Due to their lateral (clonal) growth, *Caulerpa* spp. often experience spatial variation in a range of environmental conditions and resources (Collado-Vides 2002). As a result, species within the genus *Caulerpa* show morphological plasticity, including varying patterns of internode production and length of fronds, e.g. for a more efficient light use, which affect the overall appearance of the plant (Collado-Vides 2002).

The seagrass and the green alga seem to have different physiological mechanisms to achieve photoprotection. The exposition of *C. nodosa* to high PAR seems to explain the larger antioxidant activity of the seagrass in comparison with *C. prolifera*, as a way to dissipate excess light energy. This has been described in the Mediterranean Sea, where *C. nodosa* typically live in shallow water (García-Sánchez et al. 2012). The green alga showed a larger content of carotenes than the seagrass, particularly in shallow water (i.e. under high irradiances), most likely to protect its photosynthetic machinery from light excess. In turn, when vegetative fragments of *C. prolifera* from 5 m were relocated at 20 m, the alga decreased its carotene content. In the particular case of the seagrass, however, the carotene content increased with depth; this is most likely a response to increase light harvesting by photosynthetic antennas under scenarios of low PAR. In turn, leaves of flowering plants have the capacity to adapt the carotene content either to improve light harvesting or to protect the photosynthetic machinery from light excess (Matsubara et al. 2009). These results, however, should be taken with caution, as we have not analysed the specific carotenes associated with each macrophyte. Moreover, we cannot link differences in antioxidant activity with varying quality and quantity of carotenes (e.g. b-carotene and lutein) and other chemical ways of excess light dissipation.

A range of human-induced perturbations may reduce the transparency of coastal waters, including sedimentation (e.g. associated with construction of infrastructures and coastal runoff) and fertilization (Burkholder et al. 2007). Decreased light regimes, where *C. nodosa* and *C. prolifera* coexist in subtidal soft bottoms, seem to clearly favour the alga in comparison with the seagrass, at least from a physiological point of view. The results of this study are therefore added to a body of literature that demonstrates the need to maintain coastal waters with a good quality status to promote seagrass conservation.

## ACKNOWLEDGEMENTS

This study was partially supported by the EU project ECOSERVEG, within the BEST initiative (Voluntary Scheme for Biodiversity and Ecosystem Services in Territories of the EU Outermost Regions and Oversees Countries and Territories, Grant nº 07.032700/2012/635752/SUB/B2). F. Tuya was supported by the MINECO 'Ramón y Cajal' programme. We thank T. Sánchez for his help during fieldwork. Two anonymous reviewers provided positive feedback on a previous draft of this paper.

## REFERENCES

Barberá C., Tuya F., Boyra A., et al. 2005. Spatial variation in the structural parameters of *Cymodocea nodosa* seagrass meadows in the Canary Islands: a multiscaled approach. Bot. Mar. 48: 122-126. http://dx.doi.org/10.1515/BOT.2005.021

Bernardeau-Esteller J., Marín-Guirao L., Sandoval-Gil J.M., et al. 2011. Photosynthesis and daily metabolic carbon balance of the invasive *Caulerpa racemosa* var. *cylindracea* (Chlorophyta: Caulerpales) along a depth gradient. Sci. Mar. 75: 803-810. http://dx.doi.org/10.3989/scimar.2011.75n4803

Betancor S., Domínguez B., Tuya F., et al. 2015. Photosynthetic performance and photoprotection of *Cystoseira humilis* (Phaeophyceae) and *Digenea simplex* (Rhodophyceae) in an intertidal rock pool. Aquat. Bot. 121: 16-25. http://dx.doi.org/10.1016/j.aquabot.2014.10.008

Blois M. 1958. Antioxidant determinations by the use of a stable free radical. Nature 181: 1199-1200.

Bradstreet R.B. 1965. The Kjeldahl method for organic Nitrogen. Academic Press, New York, 239 pp.

Burkholder J.M., Tomasko D., Touchette B.W. 2007. Seagrasses and eutrophication. J. Exp. Mar. Biol. Ecol. 350: 46-72. http://dx.doi.org/10.1016/j.jembe.2007.06.024

Cabello-Pasini A., Abdala-Díaz R., Macías-Carranza V., et al. 2015. Effect of irradiance and nitrate levels on the relationship between gross photosynthesis and electron transport rate in the seagrass *Cymodocea nodosa*. Cienc. Mar. 41: 93-105. http://dx.doi.org/10.7773/cm.v41i2.2499

Ceccherelli G., Cinelli F. 1997. Short-term effects of nutrient enrichment of the sediment and interactions between the seagrass *Cymodocea nodosa* and the introduced green alga *Caulerpa taxifolia* in a Mediterranean bay. J. Exp. Mar. Biol. Ecol. 217: 165-177. http://dx.doi.org/10.1016/S0022-0981(97)00050-6

Collado-Vides L. 2002. Morphological plasticity of *Caulerpa prolifera* (Caulerpales, Chlorophyta) in relation to growth form in a coral reef lagoon. Bot. Mar. 45: 123-129. http://dx.doi.org/10.1515/BOT.2002.013

Collier C.J., Waycott M., Giraldo Ospina A. 2012. Responses of four Indo-West Pacific seagrass species to shading. Mar. Poll. Bull. 65: 342-354. http://dx.doi.org/10.1016/j.marpolbul.2011.06.017

Duarte C.M., Dennison W.C., Orth R.J., et al. 2008. The charisma of coastal ecosystems. Estuar. Coasts 31: 233-238. http://dx.doi.org/10.1007/s12237-008-9038-7

García-Sánchez S., Korbee N., Pérez-Ruzafa I.M., et al. 2012. Physiological response and photoacclimation capacity of *Caulerpa prolifera* (Forsskål) J.V. Lamouroux and *Cymodocea nodosa* (Ucria) Ascherson meadows in the Mar Menor lagoon (SE Spain). Mar. Environ. Res. 79: 37-47. http://dx.doi.org/10.1016/j.marenvres.2012.05.001

Gardner A., Tuya F., Lavery P.S., et al. 2013. Habitat preferences of macroinvertebrate fauna among seagrasses with varying structural forms. J. Exp. Mar. Biol. Ecol. 439: 143–151. http://dx.doi.org/10.1016/j.jembe.2012.11.009

Grzymski J., Johnsen G., Sakshaug E. 1997. The significance of intracellular self-shading on the bio-optical properties of brown, red and green macroalgae. J. Phycol. 33: 408-414. http://dx.doi.org/10.1111/j.0022-3646.1997.00408.x

Häder D.P., Porst M., Herrmann H., et al. 1997. Photosynthesis of Mediterranean green alga *Caulerpa prolifera* measured in the field under solar irradiation. J. Photoch. Photobio. B 37: 66-73. http://dx.doi.org/10.1016/S1011-1344(96)07338-1

Hanelt D. 1998. The capability for dynamic photoinhibition in Arctic macroalgae is related to their depth distribution. Mar. Biol. 131: 361-369. http://dx.doi.org/10.1007/s002270050329

Jassby A., Platt T. 1976. Mathematical formulation of the relationship between photosynthesis and light for phytoplankton. Limnol. Oceanogr. 21: 540-547. http://dx.doi.org/10.4319/lo.1976.21.4.0540

Lapointe B.E., Barile P.J., Littler M.M., et al. 2005. Macroalgal blooms on southeast Florida coral reefs: II. Cross-shelf discrimination of nitrogen sources indicates widespread assimilation of sewage nitrogen. Harmful Algae 4: 1106-1122. http://dx.doi.org/10.1016/j.hal.2005.06.002

Lloret J., Marin A., Marin-Guirao L., et al. 2005. Changes in macrophytes distribution in a hypersaline coastal lagoon associated with the development of intensively irrigated agriculture.

Ocean. Coast. Manage. 48: 828-842. http://dx.doi.org/10.1016/j.ocecoaman.2005.07.002
Lüning K. 1990. Seaweeds: their environment, biogeography, and ecophysiology. Wiley-Interscience, New York, NY.
Malta E.J., Ferreira D.G., Vergara J.J., et al. 2005. Nitrogen load and irradiance affect morphology, photosynthesis and growth of *Caulerpa prolifera* (Bryopsidales, Chlorophyta). Mar. Ecol. Prog. Ser. 298: 101-114. http://dx.doi.org/10.3354/meps298101
Matsubara S., Krause G.H., Aranda J., et al. 2009. Sun-shade patterns of leaf carotenoid composition in 86 species of neotropical forest plants. Funct. Plant Biol. 36: 20-36. http://dx.doi.org/10.1071/FP08214
Maxwell K., Johnson G. 2000. Chlorophyll fluorescence—a practical guide. J. Exp. Bot. 51: 659-668. http://dx.doi.org/10.1093/jexbot/51.345.659
Murphy J., Riley J.P. 1962. A modified single solution method for the determination of phosphate in natural waters. Anal. Chem. Acta 27: 31-36. http://dx.doi.org/10.1016/S0003-2670(00)88444-5
Olesen B., Enríquez S., Duarte C.M., et al. 2002. Depth-acclimation of photosynthesis, morphology and demography of *Posidonia oceanica* and *Cymodocea nodosa* in the Spanish Mediterranean Sea. Mar. Ecol. Prog. Ser. 236: 89-97. http://dx.doi.org/10.3354/meps236089
Parsons T.R., Strickland J.D.H. 1963. Discussion of spectrophometric determination of marine-plant pigments, with revised equations for ascertaining chlorophyll-*a* and carotenois. J. Mar. Res. 21: 105-156.
Platt T., Gallegos I. 1980. Modelling primary production. In: Falkowski P.G. (ed.), Primary productivity in the sea. Plenum, pp. 339-351. http://dx.doi.org/10.1007/978-1-4684-3890-1_19
Raniello R., Lorenti M., Brunet C., et al. 2006. Photoacclimation of the invasive alga *Caulerpa racemosa* var. *cylindracea* to depth and daylight patterns and a putative new role for siphonoxanthin. Mar. Ecol. 27: 20-30. http://dx.doi.org/10.1111/j.1439-0485.2006.00080.x
Silva J., Barrote J., Costa M.M., et al. 2013. Physiological responses of *Zostera marina* and *Cymodocea nodosa* to light-limitation stress. PLoS ONE 8(11): e81058. http://dx.doi.org/10.1371/journal.pone.0081058
Terrados J., Ros J.D. 1992. Growth and primary production of *Cymodocea nodosa* (Ucria) Ascherson in a Mediterranean coastal lagoon: The Mar Menor (SE Spain). Aquat. Bot. 43: 63-74. http://dx.doi.org/10.1016/0304-3770(92)90014-A
Tuya F., Martín J.A., Luque A. 2006. Seasonal cycle of a *Cymodocea nodosa* seagrass meadow and of the associated ichthyofauna at Playa Dorada (Lanzarote, Canary Islands, eastern Atlantic). Cien. Mar. 32: 695-704.
Tuya F., Hernández-Zerpa H., Espino F., et al. 2013a. Drastic decadal decline of the seagrass *Cymodocea nodosa* at Gran Canaria (Eastern Atlantic): interactions with the green alga *Caulerpa prolifera*. Aquat. Bot. 105: 1-6. http://dx.doi.org/10.1016/j.aquabot.2012.10.006
Tuya F., Viera-Rodríguez M.A., Guedes R., et al. 2013b. Seagrass responses to nutrient enrichment depend on clonal integration, but not flow-on effects on associated biota. Mar. Ecol. Prog. Ser. 490: 23-35. http://dx.doi.org/10.3354/meps10448
Tuya F., Ribeiro-Leite L., Arto-Cuesta N., et al. 2014. Decadal changes in the structure of *Cymodocea nodosa* seagrass meadows: Natural vs. human influences. Estuar. Coast. Shelf Sci. 137: 41-49. http://dx.doi.org/10.1016/j.ecss.2013.11.026
Tuya F., Betancor S., Viera-Rodríguez M.A., et al. 2015. Effect of chronic versus pulse perturbations on a marine ecosystem: integration of functional responses across organization levels. Ecosystems 18: 1455-1471. http://dx.doi.org/10.1007/s10021-015-9911-8
Underwood A.J. 1997. Experiments in Ecology: their logical design and interpretation using Analysis of Variance. Cambridge Univ. Press., Cambridge, UK.
Walkley A., Black J.A. 1934. An examination of the Degtjareff method for determining soil organic matter and a proposed modification of the chromic titration method. Soil Sci. 37: 29-38. http://dx.doi.org/10.1097/00010694-193401000-00003

## APPENDICES

Appendix 1. – Sediment characteristics across depth at Gando Bay (Gran Canaria Island). Only the $P_{total}$ showed a significant change with depth.

| | 5 m | | 10 m | | 15 m | | 20 m | |
|---|---|---|---|---|---|---|---|---|
| | Mean | SD | Mean | SD | Mean | SD | Mean | SD |
| $N_{total}$ (mg $kg^{-1}$) | 405.50 | 19.09 | 251.00 | 39.60 | 307.50 | 60.10 | 403.50 | 177.48 |
| $P_{total}$ (mg $kg^{-1}$), $R^2$=0.58, P<0.01 | 1375.20 | 1669.20 | 29.95 | 9.12 | 57.20 | 11.46 | 55.25 | 41.65 |
| Organic matter (%) | 1.05 | 0.07 | 0.90 | 0.14 | 0.75 | 0.07 | 0.95 | 0.07 |
| $D_{50}$ | 0.14 | 0.00 | 0.33 | 0.25 | 0.19 | 0.02 | 0.14 | 0.00 |
| Type of sediment | Fine sands | Fine sands | Fine sands | Fine sands | Fine sands | Fine sands | Fine sands | Fine sands |

Appendix 2. – Photosynthetic parameters of *Cymodocea nodosa* and *Caulerpa prolifera* at the start of transplants (means and SE are included, n=6).

| Time | Species | Depth | $F_v/F_m$ | SE | $ETR_{max}$ | SE | $\alpha_{ETR}$ | SE | $E_k$ | SE |
|---|---|---|---|---|---|---|---|---|---|---|
| February (2014) | *C. nodosa* | 5 m | 0.824 | 0.003 | 16.490 | 1.760 | 0.097 | 0.009 | 173.156 | 24.342 |
| February (2014) | *C. prolifera* | 5 m | 0.683 | 0.021 | 11.972 | 1.354 | 0.061 | 0.009 | 196.070 | 13.459 |
| February (2014) | *C. nodosa* | 20 m | 0.823 | 0.007 | 16.583 | 1.956 | 0.112 | 0.006 | 150.331 | 25.888 |
| February (2014) | *C. prolifera* | 20 m | 0.807 | 0.009 | 13.278 | 1.509 | 0.084 | 0.008 | 157.577 | 7.494 |
| May (2014) | *C. nodosa* | 5 m | 0.747 | 0.007 | 21.394 | 1.826 | 0.118 | 0.016 | 183.970 | 17.979 |
| May (2014) | *C. prolifera* | 5 m | 0.484 | 0.111 | 10.298 | 1.828 | 0.041 | 0.002 | 244.082 | 37.737 |
| May (2014) | *C. nodosa* | 20 m | 0.772 | 0.011 | 24.361 | 1.711 | 0.141 | 0.006 | 171.441 | 5.138 |
| May (2014) | *C. prolifera* | 20 m | 0.507 | 0.155 | 8.554 | 0.703 | 0.048 | 0.009 | 184.985 | 25.912 |

Appendix 3. – Photosynthetic parameters of *Cymodocea nodosa* and *Caulerpa prolifera* at the end of transplants (means and SE are included, n=6).

| Time | Depth | Species | Origin | $ETR_{max}$ | SE | $\alpha_{ETR}$ | SE | $E_k$ | SE |
|---|---|---|---|---|---|---|---|---|---|
| February (2014) | 5 m | *C. nodosa* | autochthonous | 11.9955 | 0.971 | 0.093 | 0.008 | 132.525 | 14.813 |
| February (2014) | 5 m | *C. nodosa* | allochthonous | 9.497 | 1.348 | 0.074 | 0.009 | 130.358 | 13.305 |
| February (2014) | 5 m | *C. prolifera* | autochthonous | 2.0471 | 0.302 | 0.034 | 0.005 | 62.445 | 9.523 |
| February (2014) | 5 m | *C. prolifera* | allochthonous | 2.331 | 0.355 | 0.028 | 0.005 | 88.765 | 11.059 |
| February (2014) | 20 m | *C. nodosa* | autochthonous | 12.372 | 1.886 | 0.083 | 0.011 | 144.726 | 13.221 |
| February (2014) | 20 m | *C. nodosa* | allochthonous | 12.160 | 2.077 | 0.089 | 0.018 | 145.925 | 19.438 |
| February (2014) | 20 m | *C. prolifera* | autochthonous | 2.944 | 0.545 | 0.058 | 0.004 | 49.609 | 7.402 |
| February (2014) | 20 m | *C. prolifera* | allochthonous | 3.003 | 0.478 | 0.058 | 0.010 | 53.016 | 2.876 |
| May (2014) | 5 m | *C. nodosa* | autochthonous | 21.693 | 0.815 | 0.152 | 0.018 | 166.486 | 11.494 |
| May (2014) | 5 m | *C. nodosa* | allochthonous | 24.528 | 2.617 | 0.104 | 0.010 | 245.268 | 40.441 |
| May (2014) | 5 m | *C. prolifera* | autochthonous | 4.034 | 0.348 | 0.042 | 0.002 | 93.517 | 3.504 |
| May (2014) | 5 m | *C. prolifera* | allochthonous | 3.102 | 0.748 | 0.021 | 0.007 | 163.744 | 25.198 |
| May (2014) | 20 m | *C. nodosa* | autochthonous | 26.498 | 1.530 | 0.139 | 0.009 | 192.115 | 12.080 |
| May (2014) | 20 m | *C. nodosa* | allochthonous | 23.191 | 2.415 | 0.134 | 0.008 | 172.505 | 16.907 |
| May (2014) | 20 m | *C. prolifera* | autochthonous | 6.390 | 1.997 | 0.054 | 0.010 | 106.208 | 20.512 |
| May (2014) | 20 m | *C. prolifera* | allochthonous | 4.419 | 0.768 | 0.064 | 0.002 | 66.974 | 9.551 |